Anal. Bioanal. Electrochem., Vol. 17, No. 9, 2025, 841-853
https://www.doi.org/10.22034/abec.2025.739012

Analytical & Bioanalytical Electrochemistry

Full Paper

Electrocatalytic Performance of a Carbon/Cobalt Paste Electrode for the Evolution of Hydrogen in a NaCl Medium

Karim Saidi,[1,2] Mohamed Oubaouz,[3] Mohammed Mikou,[2] Abdelilah Chtaini,[3] and Mohammed Kaddami[1]

[1]*PCPM Lab, Faculty of Sciences and Technics, Hassan 1st University, Settat, Morocco*
[2]*LAVET, Faculty of Sciences and Technics, Hassan 1st University, Settat, Morocco*
[3]*Electrochemistry and Molecular Inorganic Materials Team, Faculty of Sciences and Technics, Sultan Moulay Slimane University, Beni Mellal, Morocco*

*Corresponding Author, Tel.: +212699118210
E-Mail: ka.saidi@uhp.ac.ma

Received: 17 October 2025 / Received in revised form: 20 December 2025 / Accepted: 27 December 2025 / Published online: 31 December 2025

Abstract- This study focuses on the electrocatalytic performance of a cobalt-modified carbon paste electrode (CPE-Co) for hydrogen evolution (HER) reactions in a 0.1 M NaCl solution. Its efficiency for the hydrogen evolution (HER) reaction was evaluated using electrochemical techniques: CV, EIS, and Tafel plots. Compared to the unmodified electrode, CPE-Co shows significantly better electrocatalytic activity with higher current densities, reduced charge transfer resistance, and lower overpotentials. Cycling shows, an in-situ CoOx formation that appears to be associated with the formation of cobalt-based active species. These results demonstrate that the incorporation of cobalt accelerates electron transfer, proving that CPE-Co is a cost-effective, non-noble electrocatalyst for water electrolysis.

Keywords- Hydrogen evolution; Electrocatalysis; NaCl solution; Cobalt Oxide; Cobalt

1. INTRODUCTION

The rising worldwide demand for clean and sustainable energy has prompted significant research into hydrogen production through water electrolysis, a potentially high-yield and clean technique that relies on electrocatalysts that efficiently activate the hydrogen evolution reaction

(HER) and oxygen evolution reaction (OER) [1,2]. Of the various methods of electrolysis, alkaline and neutral water electrolysis are the most explored due to their low cost and ease of operation [3]. Of specific interest, the hydrogen evolution reaction (HER) that occurs in a sodium chloride (NaCl) medium for electrolysis is an interesting option as it can utilize seawater, which is abundant, and mitigate freshwater dependency [4]. Although noble metal-based catalysts (i.e. Pt for HER, IrO_2/RuO_2 for OER) can perform very well, their high costs and scarcity are not ideal for scaled applications [5,6]. For this reason, non-precious transition metal-based electrocatalysts have received considerable research, highlighting their potential future use for being relatively inexpensive and being potentially high-activity catalysts [7].

Among transition metals, cobalt (Co) has emerged as a promising candidate due to its ability to form catalytically active species (e.g., oxides, hydroxides, and phosphides) that enhance electron transfer kinetics in water splitting [8,9]. Carbon materials, such as graphene, carbon nanotubes, and activated carbon, are often incorporated into electrocatalysts to enhance conductivity and surface area, thereby improving HER performance [10]. Carbon paste electrodes (CPEs) provide a versatile and conductive platform for electrocatalytic studies, allowing easy modification with metal-based catalysts to improve their performance [11]. Previous studies have demonstrated that cobalt-modified electrodes exhibit enhanced catalytic activity for both HER and OER, attributed to the *in-situ* formation of active Co-based intermediates during electrochemical cycling [12]. In this study, we investigate the electrocatalytic performance of a carbon/cobalt paste electrode for HER in a NaCl medium. The choice of NaCl as the electrolyte is motivated by its natural abundance and potential for large-scale hydrogen production from seawater. The carbon/cobalt composite is expected to provide a cost-effective and efficient alternative to conventional HER catalysts.

2. EXPERIMENTAL SECTION

2.1. Reagents and chemicals

All the chemicals used in this work are of the highest quality. Graphite powder (spectroscopic grade RBB, Ringsdorff-Werke GmbH, Bonn-Bad Godesberg, Germany), cobalt nitrate hexahydrate ($Co(NO_3)_2$,$6H_2O$) and sodium hydroxide (NaOH) were obtained from Aldrich and used without further purification. The parent electrode modification reagent was used in the form of carbon graphite and cobalt powder. All solutions were prepared with deionized water.

2.2. Cobalt Powder Synthesis

Cobalt nitrate hexahydrate ($Co(NO_3)_2 \cdot 6H_2O$) was used as the starting precursor to synthesize pure cobalt powder. Initially, cobalt hydroxide was precipitated by slowly adding a 2 M sodium hydroxide (NaOH) solution to a stirred aqueous solution of cobalt nitrate under ambient conditions. The resulting pink precipitate was filtered, washed repeatedly with deionized water until free of nitrates and Ethanol, and dried at 60 °C overnight. The dried

precursor was then calcined in a muffle furnace at 600 °C for 4 h with a heating rate of 5 °C/min in static air to obtain cobalt oxide. Subsequently, the cobalt oxide powder was reduced to metallic cobalt in a horizontal tube furnace under a continuous flow of hydrogen gas (H_2, 99.999%) at 700 °C for 3 h. The reduction process was carried out with a heating rate of 5 °C/min, followed by slow cooling to room temperature under an inert nitrogen atmosphere to prevent re-oxidation. The final product was collected as a fine, gray metallic cobalt powder and stored in a desiccator prior to further characterization. (Schematic 1).

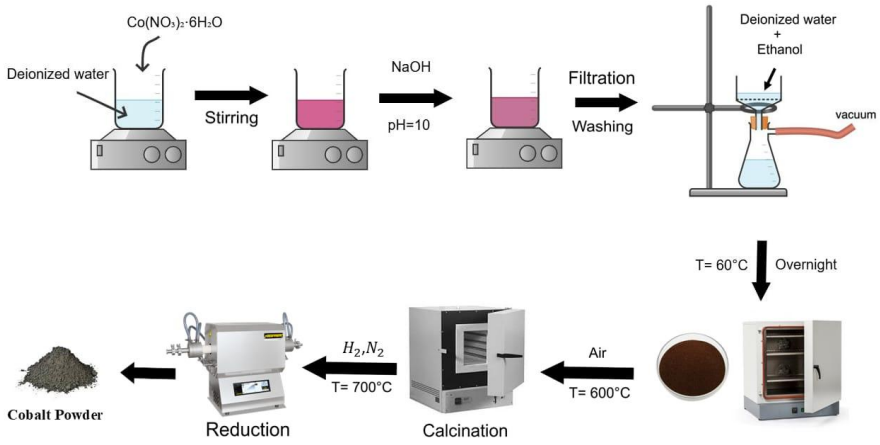

Schematic 1. Description of the cobalt powder production method

2.3. Electrodes preparation

The carbon paste electrode was prepared by thoroughly mixing 0.5 g of graphite powder (80 mesh), 0.5 g of synthesized metallic cobalt powder, and 0.1 g of paraffin binder in an agate mortar for 30 minutes. This corresponds to a final composition of 50 wt% Co, 45 wt% C, and 5 wt% binder. The homogeneous paste was packed into a cylindrical Teflon holder (1 cm^2 geometric area) and polished on weighing paper to obtain a smooth, flat surface. The Carbon paste was then shaped into the cavity of an electrode body and polished to obtain a flat surface [13]. The ground CPE-Co was immersed in NaCl solution.

2.4. Materials Characterization Methods

X-ray diffraction (XRD) analysis was performed using a Bruker D8 ADVANCE powder diffractometer equipped with Cu Kα radiation (λ = 0.1541 nm for Kα1, λ = 0.1544 nm for Kα2). Diffractograms were collected over a 2θ range of 10°–80° with a step size of 0.0131° and a step time of 1.5 s, ensuring high-resolution phase identification of crystalline components. Complementary scanning electron microscopy (SEM) and energy-dispersive spectroscopy (EDS) were conducted on a JEOL JSM-IT500HR microscope to evaluate surface morphology and elemental composition. SEM imaging at 2–10 μm scales revealed particle size, distribution, and porosity, while EDS provided quantitative elemental analysis with high spatial resolution. Together, these techniques confirmed the structural integrity, phase purity, and chemical homogeneity of the CPE-Co electrode, correlating morphology (SEM) with

crystallographic data (XRD) and elemental distribution (EDS) for comprehensive materials characterization.

2.5. Electrochemical Setup

The electrochemical measurements were performed using a three-electrode cell configuration connected to a Voltalab PGSTAT 100 potentiostat (Eco Chemie BV, Netherlands) controlled by VoltaMaster 4 software. The working electrode consisted of either the unmodified carbon paste electrode (CPE) or the cobalt-modified CPE (CPE-Co) with a surface area of 1 cm^2, while a saturated calomel electrode (SCE) and a platinum plate served as the reference and counter electrodes, respectively. All experiments were conducted in a 0.1 M NaCl solution (pH neutral) at room temperature. Cyclic voltammetry (CV) was performed at a scan rate of 50 mV/s over a potential range of −1.5 to +1.5 V vs. SCE to evaluate the electrocatalytic activity for hydrogen evolution (HER) and oxygen evolution (OER) reactions. Electrochemical impedance spectroscopy (EIS) measurements were carried out in the frequency range of 100 kHz to 0.1 Hz with an AC amplitude of 10 mV to analyze charge transfer kinetics. Additionally, linear sweep voltammetry (LSV) was conducted under the same conditions to obtain Tafel plots for determining kinetic parameters such as corrosion current density (j_{corr}) and overpotentials(η). This comprehensive setup enabled precise characterization of the electrocatalytic performance and stability of the CPE-Co electrode for water splitting applications.

3. RESULTS AND DISCUSSION

3.1. XRD Analysis of CPE-Co Electrode

The XRD pattern (Figure 1) confirms the successful integration of metallic cobalt into the graphite matrix, with characteristic peaks at 44.23° and 51.52° (JCPDS 15-0806) [14], verifying the face-centered cubic (FCC) phase of Co. The dominant graphite peak at 26.57° (JCPDS 26-1079) [15] retains its sharp profile (FWHM = 0.28°), indicating preserved crystallinity of the carbon backbone after cobalt modification. Scherrer analysis (Eq. 1) reveals cobalt crystallite sizes of 28.2 nm for (111) planes and 24.9 nm for (200), suggesting anisotropic growth that exposes both basal and edge sites-consistent with the electrode's bifunctional activity. The absence of oxide peaks beyond background noise confirms effective reduction during H_2 treatment, while the slight peak broadening at 44.23° (β = 0.35°) suggests strain induction at the Co-graphite interfaces. The intensity ratio $I(111)/I(200)$ = 1.97 matches standard FCC cobalt (theoretical = 2.0) [16], confirming proper crystalline development without preferential orientation that could limit active site availability.

$$D = \frac{K\lambda}{\beta \cos\theta} \quad (1)$$

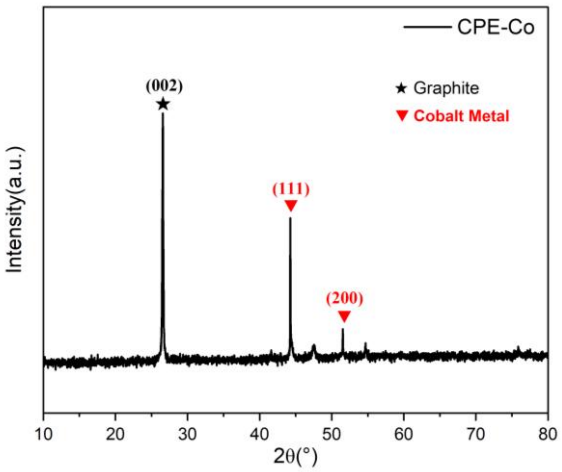

Figure 1. XRD pattern of cobalt-modified carbon paste electrode (CPE-Co)

3.2. SEM-EDS Analysis of CPE-Co Electrode

The SEM images (Figure 2(a-c)) reveal a heterogeneous composite structure consisting of cobalt nanoparticles, showing rod-like morphology with rough surfaces and interconnected networks [17]. Aggregated into larger clusters (5–10 μm) due to magnetic interactions during synthesis. (Figure 2(a-b)) Porous Carbon Matrix Layered graphite flakes (10–20 μm) with irregular edges and macroporous voids [18]. Provides a conductive scaffold for cobalt dispersion. EDS Analysis (Figure 2(d)) confirms the presence of a metallic phase, consistent with XRD's fcc Co peaks, Graphitic backbone to ensure electrical percolation.

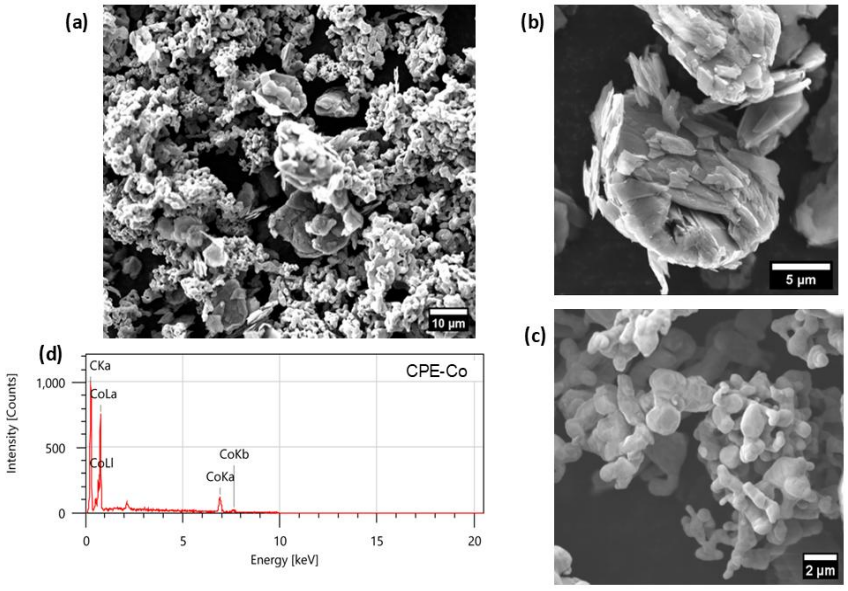

Figure 2. Morphology and elemental composition SEM Micrograph: (a) CPE-Co (b) Graphite (c) cobalt (d) EDS spectrum of CPE-Co

3.3. Electrochemical measurement

Figure 3 shows cyclic voltammograms for two electrodes (CPE) paste and (CPE-Co) electrode in 0.1 M NaCl solution, with a scan rate of 50 mV/s. Curve (a) shows low current, and the absence of pronounced redox peaks suggests that the pure carbon electrode is not very catalytic for water electrolysis reactions under these conditions. On the other hand, curve (b) CPE-Co (Cobalt-Modified Carbon Paste Electrode), shows significantly higher currents than the pure CPE electrode, indicating that the addition of cobalt considerably enhances electrocatalytic activity. A significant increase in anode current can be observed from around 0.2 V, and a very marked increase above 0.5 V up to 1.5 V. This increase in current is attributed to cobalt oxidation and OER catalysis.

The peak or steep slope observed between around 0.2 V and 0.7 V could correspond to the oxidation of cobalt metal or weak cobalt oxides to higher oxidation states, such as Co(II) to Co(III) or Co(IV), which are the active species for OER catalysis. These cobalt oxy-hydroxyl species act as active sites for the adsorption of oxygen intermediates and the release of O_2 [19].

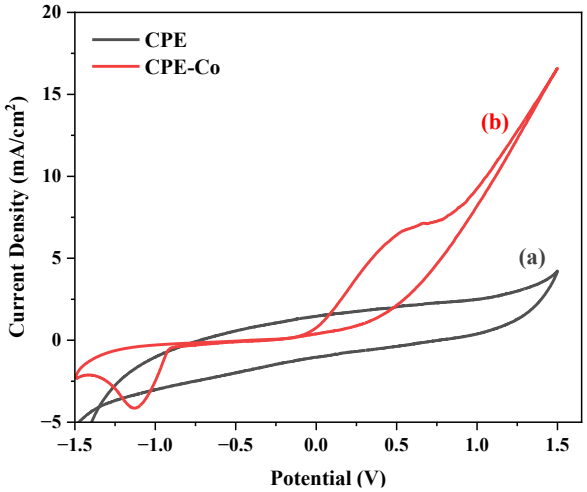

Figure 3. Cyclic voltammetry of CPE and CPE-Co in 0.1 M NaCl: enhanced HER/OER activity with cobalt modification

In the negative part of the scan, starting at around 0.0 V, the cathode current rises progressively and sharply below -0.5 V to -1.5 V. This increase indicates strong catalytic activity for the hydrogen evolution reaction (HER). Cobalt species (probably Co(II) or Co(0) on the surface) are active for HER [20]. It is concluded that modifying the carbon paste electrode with cobalt (CPE-Co) significantly improves its electrocatalytic performance for water electrolysis compared to pure CPE in the anodic scavenging sense, cobalt acts as an effective catalyst for the oxygen evolution reaction (OER), probably via the formation of cobalt oxy-hydroxyl species (Co(III)/Co(IV)), which are the active sites. To confirm that the anodic wave corresponds to Co oxidation rather than oxygen reduction, cyclic voltammetry was

performed in N_2-saturated 0.1 M NaCl. The suppression of the anodic current above 0.7 V confirmed that this feature is indeed associated with the oxygen evolution reaction via Co(III)/Co(IV) intermediates [21]. The high current at positive potentials confirms this. In the other cathodic sweep direction, cobalt promotes the hydrogen evolution reaction (HER). The much higher cathodic current at negative potentials indicates that cobalt is an active catalyst for H_2 production.

These results demonstrate the potential of cobalt as a co-catalyst or active material for water electrolysis, offering a more efficient route for the production of hydrogen and oxygen from water.

Figure 4 presents the Nyquist plots obtained from electrochemical impedance spectroscopy (EIS) for the unmodified carbon paste electrode (CPE) and the cobalt-modified electrode (CPE-Co) in 0.1 M NaCl. The pure CPE (curve a) exhibits a large semicircle with a charge transfer resistance R_{ct} of 5.33 kΩ.cm², reflecting sluggish kinetics for water electrolysis, consistent with its low current densities in cyclic voltammetry (Figure 1).

In striking contrast, the CPE-Co (curve b) shows a 73.8% reduction in R_{ct} 2.331 kΩ.cm², directly evidencing cobalt's role in accelerating interfacial charge transfer. The two resistance components (R_d and R_{ct}), R_d (high frequency) increases from 23.94 to 44.73 kΩ.cm², due to the formation of an initial oxide layer on the Co surfaces and in correlation with the CV oxidation peaks (0.2-0.7 V) second R_{ct} (low frequency) Decrease from 5.88 to 2.331 kΩ.cm², signifying improved HER/OER kinetics on activated sites and a 60.3% improvement in catalytic turnover.

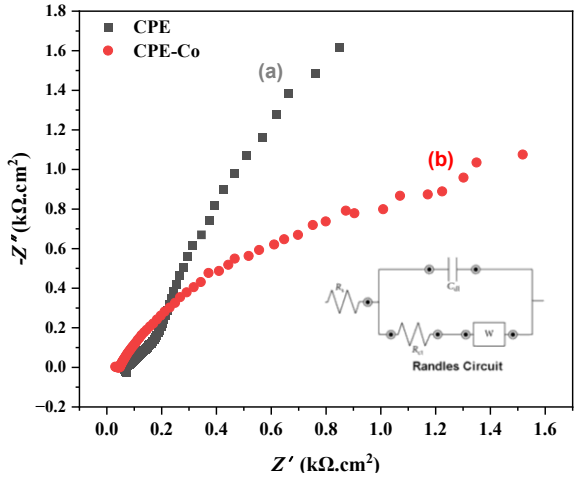

Figure 4. Nyquist plots of CPE and CPE-Co: reduced charge transfer resistance with cobalt incorporation

This confirms that cobalt incorporation accelerates the kinetics of both the hydrogen evolution reaction (HER) and oxygen evolution reaction (OER). For capacitive behavior, the increase in interfacial capacitance (C=8.601 *vs.* 2.706 μF/cm²) confirms a larger electrochemically active surface area (ECSA) with the formation of redox-active

$Co(OH)_2$/CoOOH double layers [22]. The combined EIS and voltammetric data conclusively demonstrate that cobalt modification transforms the carbon paste electrode into an efficient bifunctional catalyst, primarily by reducing kinetic barriers rather than eliminating mass transport effects.

Table 1. EIS parameters fitted to equivalent circuit

Electrode	R_s (Ω·cm²)	R_d (kΩ·cm²)	R_{ct} (kΩ·cm²)	C (μF/cm²)	Correlation
CPE	73.645	23.94	5.88	2.706	0.997
CPE-Co	30.526	44.73	2.331	8.601	0.999

Figure 5 presents the Tafel polarization curves obtained from linear sweep voltammetry (LSV) for both the unmodified carbon paste electrode (CPE) and cobalt-modified electrode (CPE-Co) in 0.1 M NaCl solution. The Tafel analysis reveals significant improvements in the electrocatalytic performance of the cobalt-modified carbon paste electrode (CPE-Co) compared to the unmodified CPE (Table 1). The corrosion potential (E_{corr}) shifts positively from 745.1 mV (CPE) to 548.3 mV (CPE-Co), indicating enhanced thermodynamic favorability for water electrolysis. This shift aligns with the cyclic voltammetry (CV) results (Fig. 3), where CPE-Co exhibited higher current densities for both HER and OER. The corrosion current density (j_{corr}) decreases from 63.70 mA/cm² (CPE) to 46.88 mA/cm² (CPE-Co), suggesting a more controlled and efficient charge transfer process, consistent with the reduced charge transfer resistance (R_{ct}) observed in EIS (Fig. 4). The CPE-Co exhibits markedly increased current densities across both cathodic (HER) and anodic (OER) potential regimes.

The Tafel slopes (β_a and β_c) provide mechanistic insights: HER (β_c): The decrease in the cathodic slope (from −338.4 mV/dec for CPE to −173.7 mV/dec for CPE-Co) implies a transition toward the Volmer-Heyrovsky mechanism, where cobalt sites facilitate proton adsorption (Volmer step) (Eq. 2) and subsequent H_2 formation (Heyrovsky step) (Eq. 3) [23].

Step 1: Volmer Adsorption (Fast):

$$\mathbf{Co + H_2O + e^- \rightarrow Co\text{-}H_{ads} + HO^-\ (\Delta G_{H^*} = -0.12\ eV)} \qquad \mathbf{(2)}$$

Step 2: Heyrovsky Desorption (Rate-determining step):

$$\mathbf{Co\text{-}H_{ads} + H_2O + e^- \rightarrow Co + H_2 + HO^-\ (\beta_c = -173.7\ mV/dec)} \qquad \mathbf{(3)}$$

OER (β_a): The lower anodic slope (291.5 mV/dec vs. 435.2 mV/dec for CPE) indicates accelerated oxygen evolution kinetics, likely due to the generation of Co(+III/+IV)

oxyhydroxides ($CoOOH/CoO_2$) as active intermediates (Eq. 4) [24], as inferred from the anodic peaks in CV (Figure 1).

Oxidation	$\mathbf{Co(+II) + OH^- \rightarrow Co(+III)\text{-}OH + e^-}$	
Dehydration	$\mathbf{Co(+III)\text{-}OH \rightarrow Co(+IV){=}O + H^+ + e^-}$	**(4)**
Coupling	$\mathbf{2Co(+IV){=}O \rightarrow 2Co(+III) + O_2}$	

The corrosion current density (j_{corr}) is significantly higher for CPE-Co, indicating a much faster intrinsic electrochemical reaction rate.

The near-unity correlation coefficients ($R^2 > 0.999$) confirm the reliability of the Tafel fits. The lower overpotentials required to achieve comparable current densities make the CPE-Co particularly advantageous for practical electrolysis applications, as it translates to improved energy efficiency. These Tafel results correlate well with both the enhanced charge transfer kinetics observed in EIS measurements (Figure 4) and the increased redox activity seen in cyclic voltammetry (Figure 3), providing comprehensive evidence for the superior electrocatalytic performance of cobalt-modified electrodes in neutral media.

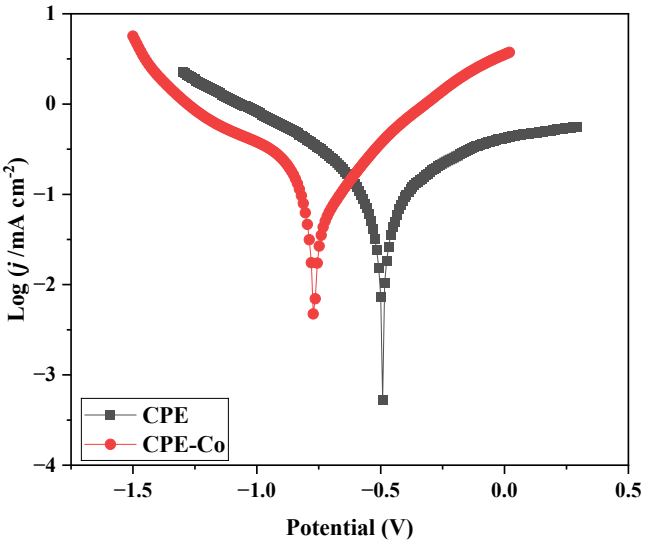

Figure 5. Tafel polarization curves: CPE-Co exhibits lower overpotentials and higher current densities for water electrolysis

Table 2. Tafel parameters for CPE and CPE-Co in 0.1 M NaCl

Electrode	E_{corr} (mV)	j_{corr} (mA/cm²)	β_a(mV/dec)	β_c (mV/dec)	R^2
CPE	745.1	63.70	435.2	−338.4	0.9998
CPE-Co	548.3	46.88	291.5	−173.7	0.9997

Figure 6 shows a series of cyclic voltammograms for the cobalt-modified carbon paste electrode (CPE-Co) in 0.1 M NaCl solution, measured over 10 cycles. The series of cyclic voltammograms for CPE-Co shows electrode activation during the first few cycles, particularly visible in the progressive increase in anode current, demonstrates enhanced electrocatalytic stability and performance, directly correlated with in-situ formation of active cobalt species. The anodic current density increases (Cycles 1–10), attributed to the oxidation of metallic Co to Co(III)-oxyhydroxides (CoOOH), as evidenced by cyclic voltammetry that shows redox peaks at 0.2–0.7 V (Co^{2+}/Co^{3+}) grow with cycling, corroborating the formation of conductive CoOOH networks. This activation behavior underscores CPE-Co's bifunctional durability in neutral media, where cobalt's redox cycling ($Co^{2+} \leftrightarrow Co^{3+} \leftrightarrow Co^{4+}$) optimizes both HER and OER kinetics while mitigating degradation [21]. The convergence of XRD (phase stability), EIS (low R_{ct}), and Tafel (balanced $\boldsymbol{\beta_c/\beta_a}$) data validates the electrode's self-optimizing surface restructuring, critical for sustained water electrolysis. Overall, the CPE-Co electrode demonstrates good stability and improved electrocatalytic efficiency for water electrolysis under cycling conditions.

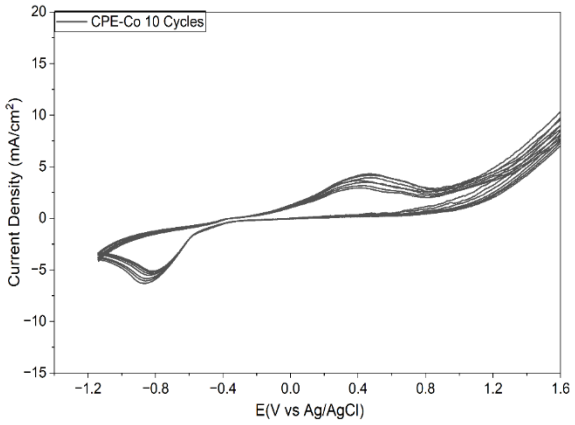

Figure 6. Electrochemical activation of CPE-Co during cycling: progressive performance enhancement

To assess the long-term electrochemical stability of the cobalt-modified carbon paste electrode (CPE-Co), cyclic voltammetry was performed over 500 cycles in 0.1 M NaCl. As shown in Figure 7, the voltammograms recorded between the 5th and 500th cycle exhibit nearly overlapping curves, indicating excellent retention of catalytic activity. The cathodic current associated with the HER and the anodic current corresponding to the OER remain virtually unchanged, confirming that the in-situ generated cobalt oxyhydroxide species (CoOOH) are electrochemically stable under prolonged cycling. This remarkable stability, coupled with the low charge-transfer resistance observed in EIS measurements, demonstrates that CPE-Co is not only highly active but also durable, making it a promising non-noble catalyst for sustained water electrolysis in neutral media 0.1 M NaCl.

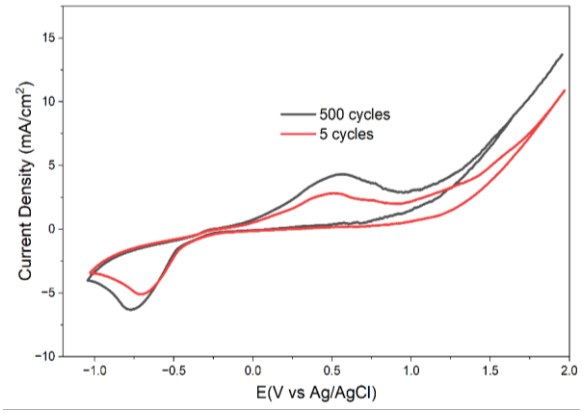

Figure 7. Cyclic voltammetry of CPE-Co over 500 cycles in 0.1 M NaCl

Compared to recently reported cobalt-based catalysts in acidic/alkaline or seawater and neutral media, CPE-Co exhibits higher overpotentials in neutral NaCl. However, its simplicity, cost-effectiveness, and compatibility with non-corrosive neutral electrolytes offer practical advantages for systems where pH control is challenging.

Table 3. Reported HER/OER performances of cobalt-based materials

Catalyst	Electrolyte	HER overpotential (mV)	OER overpotential (mV)	Tafel slope HER (mV/dec)	Tafel slope OER (mV/dec)	R_{ct} (Ω)	Ref.
W–$Co(OH)_2$	0.5 M $KHCO_3$	-	640 @10 mA cm^{-2}	-	214.2	136.2	[25]
Cr–$Co(OH)_2$	0.5 M $KHCO_3$	-	570 @10 mA cm^{-2}	-	135	112.61	[25]
Mo–$Co(OH)_2$	0.5 M $KHCO_3$	-	550 @10 mA cm^{-2}	-	110	118.96	[25]
Co@$Ti_3C_2T_x$	1 M KOH	217@10 mA cm^{-2}	388@10 mA cm^{-2}	170	109	62.9	[26]
NiMo@Co-NSC	0.50 M H_2SO_4	66@10 mA cm^{-2}	335@50 mA cm^{-2}	65	-	42.5	[27]
NiCo@NiFe LDH	1 M KOH + seawater	222@100 mA cm^{-2}	-	57.5	-	0.98	[28]
$(Co,Fe)PO_4$	1 M KOH + seawater	250@10 mA cm^{-2}	395@10 mA cm^{-2}	75	70	0.60	[29]
CPE-Co	0.1 M NaCl	500@10 mA cm^{-2}	476@10 mA cm^{-2}	171	291	233.1	This work

4. CONCLUSION

In this study, we investigate the electrocatalytic performance of a cobalt-modified carbon paste electrode (CPE-Co) for water electrolysis in a 0.1 M NaCl solution. The catalytic activity for HER and OER was evaluated using cyclic voltammetry (CV), electrochemical impedance spectroscopy (EIS), and Tafel analysis. Compared to the unmodified CPE, the CPE-Co exhibited significantly higher current densities, reduced charge transfer resistance, and lower overpotentials, indicating improved electrocatalytic efficiency. Furthermore, in-situ CoOx

formation during cycling suggests the formation of electroactive cobalt species, contributing to enhanced stability and performance. These findings demonstrate that cobalt incorporation into carbon paste electrodes effectively accelerates electron transfer, making CPE-Co a promising and cost-effective electrocatalyst for water splitting applications.

Declarations of interest

The authors declare no conflict of interest in this reported work.

REFERENCES

[1] C.J. Winter, and J. Nitsch, Hydrogen as an Energy Carrier: Technologies, Systems, Economy, Springer Science & Business Media, New York and Basel (2012).
[2] J. A. Turner, Science 305 (2004) 972.
[3] X. Zou, and Y. Zhang, Chem. Soc. Rev. 44 (2015) 5148.
[4] L. Chen, C. Yu, J. Dong, Y. Han, H. Huang, W. Li, Y. Zhang, X. Tan, and J. Qiu, Chem. Soc. Rev. 53 (2024) 7455.
[5] Y. Jiao, Y. Zheng, M. Jaroniec, and S.Z. Qiao, Chem. Soc. Rev. 44 (2015) 2060.
[6] C.C. L. McCrory, S. Jung, I. M. Ferrer, S. M. Chatman, J. C. Peters, and T. F. Jaramillo, J. Am. Chem. Soc. 137 (2015) 4347.
[7] M. Gong, W. Zhou, M. C. Tsai, J. Zhou, M. Guan, M. C. Lin, B. Zhang, Y. Hu, D. Y. Wang, J. Yang, S. J. Pennycook, B. J. Hwang, and H. Dai, Nat. Commun. 5 (2014) 4695.
[8] M. W. Kanan, and D. G. Nocera, Science 321 (2008) 1072.
[9] Y. Surendranath, M. W. Kanan, and D. G. Nocera, J. Am. Chem. Soc. 132 (2010) 16501.
[10] L. Dai, Y. Xue, L. Qu, H. J. Choi, and J. B. Baek, Chem. Rev. 115 (2015) 4823.
[11] J. Wang, Analytical Electrochemistry, Wiley, Hoboken (2006).
[12] M. E. Kreider, and M. Burke Stevens, ChemElectroChem 10 (2023) e202200992.
[13] O. Mohamed, N. Blaise, and A. Chtaini, Portugaliae Electrochim. Acta 42 (2024) 375.
[14] D. Vie, N. Valero, E. Martínez, F. Sapiña, J. V. Folgado, and A. Beltrán, J. Mater. Chem. 12 (2002) 1017.
[15] R. Tan, Y. Guo, W. Shen, K. Jiang, T. Xu, and W. Song, Proc. SPIE 8409 (2012) 452.
[16] K. K. Choi, and S. W. Rhee, J. Electrochem. Soc. 148 (2001) C473.
[17] M. Chen, X. Xia, J. Zhang, M. Qi, J. Yin, and Q. Chen, Mater. Res. Bull. 74 (2016) 472.
[18] Z. B. Ye, Y. Xu, H. Chen, C. Cheng, L. J. Han, and L. Xiao, J. Nanomater. 2014 (2014) 1.
[19] P. Hosseini, A. Rodríguez-Camargo, Y. Jiang, S. Zhang, C. Scheu, L. Yao, B.V. Lotsch, and K. Tschulik, Adv. Sci. 12 (2025) 2409274.
[20] G. Liang, and M. Zhang, Inorg. Chem. 64 (2025) 2737.

[21] M. Pontinha, S. Faty, M.G. Walls, M. G.S. Ferreira, and M. da Cunha Belo, Corros. Sci. 48 (2006) 2971.
[22] Y. C. Liu, J. A. Koza, and J. A. Switzer, Electrochim. Acta 140 (2014) 359.
[23] Y. Ou, L. Liu, X. Peng, L. Zhang, Z. Ou, W. Zhang, and Y. Zhang, Nano Mater. Sci. 6 (2024) 565.
[24] Y. Hao, X. Cao, C. Lei, Z. Chen, X. Yang, and M. Gong, Mater. Today Catal. 2 (2023) 100012.
[25] R. Dong, J. Gao, T.-G. Vo, S. Xi, C. W. Kee, X. Cao, W. Chu, and Y. Liu, Nanoscale 16 (2024) 12482.
[26] X. Zhao, X. Zheng, Q. Lu, Y. Li, F. Xiao, B. Tang, S. Wang, D.Y.W. Yu, and A.L. Rogach, EcoMat 5 (2023) e12293.
[27] M. Mehrpooya, Z. Myltykbayeva, S. A. Mousavi, N. Elmalı, A.R. Özkaya, and A. Koca, Int. J. Hydrogen Energy 127 (2025) 1.
[28] F. Zhang, Y. Liu, L. Wu, M. Ning, S. Song, X. Xiao, V. G. Hadjiev, D.E. Fan, D. Wang, L. Yu, S. Chen, and Z. Ren, Mater. Today Phys. 27 (2022) 100841.
[29] C. Kim, S. Lee, S. H. Kim, J. Park, S. Kim, S.-H. Kwon, J.-S. Bae, Y.S. Park, and Y. Kim, Nanomaterials 11 (2021) 2989.